Chemosphere 256 (2020) 127063

Contents lists available at ScienceDirect

Chemosphere

journal homepage: www.elsevier.com/locate/chemosphere

Impact of dispersant on crude oil content of airborne fine particulate matter emitted from seawater after an oil spill

Nima Afshar-Mohajer [a, b], Andres Lam [a], Lakshmana Dora [c], Joseph Katz [c], Ana M. Rule [a], Kirsten Koehler [a, *]

[a] Department of Environmental Health and Engineering, Johns Hopkins Bloomberg School of Public Health, Baltimore, MD, USA
[b] Gradient Corporation, Boston, MA, USA
[c] Department of Mechanical Engineering, Johns Hopkins University, Baltimore, MD, USA

HIGHLIGHTS

- Use of dispersant increases the crude oil content of airborne PM after an oil spill.
- Dispersant to oil ratio as sprayed onto the slick was restored in airborne fine PM.
- The crude oil concentration of $PM_{2.5}$ increases 8.83 × at DOR 1:25.
- The finer the PM, the higher the total concentration of airborne crude oil.

GRAPHICAL ABSTRACT

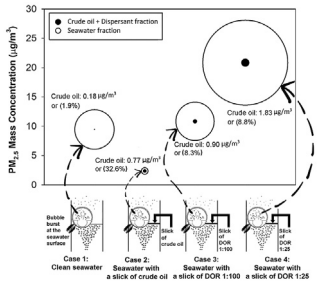

ARTICLE INFO

Article history:
Received 11 February 2020
Received in revised form
10 May 2020
Accepted 11 May 2020
Available online 19 May 2020

Handling Editor: Keith Maruya

Keywords:
Corexit 9500A
Crude oil
GC/MS
Bubble bursting
Low-pressure cascade impactor

ABSTRACT

Inhalation of $PM_{2.5}$, particles with an aerodynamic diameter <2.5 μm, from sea spray after crude oil spills could present serious health concerns. The addition of dispersants to effectively spread the crude oil throughout the water column has been practiced in recent years. Here, we investigated the possibility of an increase in the toxic content of fine PM after adding dispersant. A laboratory setup consisted of a vertical tank filled with seawater, 31.5 L airspace for aerosol sampling, and a bubble generating nozzle that aerosolized the oily droplets. Four different cases were studied: no slick, 0.5-mm-thick slick of pure crude oil (MC252 surrogate), dispersant (Corexit 9500A) mixed with crude oil at dispersant to oil ratio (DOR) 1:25, and DOR 1:100. The resulting airborne droplets were sampled for gravimetric and chemical analyses through development of a gas chromatography and mass spectrometry technique. Also, $PM_{2.5}$ particles were size-fractioned into 13 size bins covering <60 nm to 12.1 μm using a low-pressure cascade impactor.

The highest $PM_{2.5}$ concentration (20.83 ± 5.21 μg/m^3) was released from a slick of DOR 1:25, 8.83× greater than the case with pure crude oil. The average ratio of crude oil content from the slick of DOR 1:25 to the case with pure crude oil was 2.37 (1.83 vs 0.77 μg/m^3) that decreased to 1.17 (0.90 vs 0.77 μg/m^3) at DOR 1:100. For particles <220 nm, the resultant crude oil concentrations were 0.64 and 0.29 μg/m^3 at DOR 1:25 and 1:100, both higher than 0.11 μg/m^3 from the slick of pure crude oil.

* Corresponding author. Department of Environmental Health and Engineering, Johns Hopkins Bloomberg School of Public Health, 615 N. Wolfe St., Baltimore, MD, 21205, USA.
E-mail addresses: nima.a-mohajer@gradientcorp.com (N. Afshar-Mohajer), kirsten.koehler@jhu.edu (K. Koehler).

https://doi.org/10.1016/j.chemosphere.2020.127063
0045-6535/

1. Introduction

From 2000 to 2019, there were1–4 large spills (>700 tons) and 2–3 medium spills (7–700 tons) of crude oil into the seawater worldwide per year (Oil Tanker Spill Statistics, 2019). Crude oil spills expose marine species and humans to numerous toxic hydrocarbons (Boylan and Tripp, 1971). Volatile- and semi-volatile organic compounds (VOCs and SVOCs) are emitted by the contaminated slick for several days after a spill (Hanna and Drivas, 1993; Avens et al., 2011). Crude oil spills leave a layer of *n*-alkane compounds on the surface that are later emitted as airborne droplets (referred to as marine aerosol or sea sprays) due to certain natural processes (Spiel and De Leeuw, 1996; Veron et al., 2012; De Leeuw et al., 2011).

Marine aerosols containing organic constituents from crude oil raise health concerns for cleanup workers and residents in nearby communities (Aguilera et al., 2010; Levy and Nassetta, 2011). It is well-known that inhalation of ambient airborne particulate matter (PM) with an aerodynamic diameter smaller than 2.5 μm ($PM_{2.5}$), particularly those with an aerodynamic diameter smaller than 100 nm (ultra-fine particles or UFP), is associated with a variety of pulmonary diseases, upper respiratory tract irritation (Kim et al., 2015; Pope and Dockery, 2006; Valavanidis et al., 2008), and disruption of systemic vascular function (Rundell et al., 2007; Schulz et al., 2005). Compared to the size fraction of $PM_{2.5}$ between 100 nm and 2.5 μm, exposure to UFP strongly impacts pulmonary function due to their greater surface area and ability to penetrate deep into the alveolar region of the lung (Oberdörster et al., 2007). A series of epidemiologic studies performed on cleanup workers engaged in major oil spills and on inhalation of oily PM demonstrated a wide range of health impacts ranging from acute symptoms, such as headache, nausea, eye, and skin irritation (Morita et al., 1999; Sim et al., 2010), to chronic symptoms persisting years after the exposure, such as leukemia (Talbott et al., 2011), changes in the blood profile (D'Andrea and Reddy, 2013), respiratory disorders (Meo et al., 2008), and infertility (Merhi, 2010). Furthermore, surface-dwelling marine mammals such as dolphins, whales, and otters are subject to health threats through inhalation of oily aerosol especially as they have up to 8 times greater air retention time in their lungs than humans (Takeshita et al., 2017; Rosenberger et al., 2017).

The application of surfactant compounds, also known as dispersants, for breaking up the crude oil slick by aerial spraying or under-water injection has been practiced and encouraged in recent years (Lessard and DeMarco, 2000; Kleindienst et al., 2015). Crude oil dispersion mechanisms via addition of dispersants have been discussed elsewhere (Riehm and McCormick, 2014; Venkataraman et al., 2013). This process introduces additional challenges in estimating the burden of the aerosolized toxic chemicals after an oil spill (Afshar-Mohajer et al., 2019). In some cases, especially in arctic regions, propeller wash was used as a means to enhance effectivity of dispersants in dispersion of the spilled oil (Zhang et al., 2010).

Aerosolization of seawater occurs when air is entrained into the water due to naturally imposed stresses such as winds and waves and is then ejected into the atmosphere (O'Dowd and De Leeuw, 2007). Turbulent shearing caused by adding dispersant into the water contaminated after an oil spill forms underwater micron-sized droplets that may become airborne due to the small interfacial tension between oil and water (Gopalan and Katz, 2010; Zhao et al., 2017). Bubble bursting is a major source of marine aerosol formation in real-world water bodies that has been simulated in laboratory studies (Fuentes et al., 2010; Resch et al., 1986; Sampath et al., 2019; Ulevicius et al., 1997). However, previous studies mostly focused on physical characterization of the aerosol; and therefore, provided minimal information about the chemical composition of the PM. Ehrenhauser et al. (2014) used an electrostatic precipitator to collect airborne droplets aerosolized from a laboratory-scaled bubble generation system in which crude oil was continuously injected at a variable rate (with or without dispersant) from the bottom of a tank. Then an energy dispersive *X*-ray spectrometer was used to explore the elemental composition of the collected particles. Results of their analysis revealed the existence of C_{20}–C_{29} alkanes found in crude oil in the aerosolized mass and that the alkanes were more abundant in the presence of a dispersant. However, the study did not control for the size of generated bubbles and focused on chemical analyses of bulk PM with diameters ranging from 0.1 to 10 μm. The airborne particle size is inversely associated with the final size of the bubbles right before bursting on the water surface (Spiel, 1997). Furthermore, there is evidence that the number concentration of airborne PM smaller than 400 nm (*i.e.*, number of particles per volume of air) only increases substantially after addition of a dispersant, thus a more careful consideration of particle size is warranted (Afshar-Mohajer et al., 2018; Liyana-Arachchi et al., 2014; Sampath et al., 2019; Sellegri et al., 2006).

The potential increase in the toxic content of submicron PM after dispersant is used compared to PM from crude oil alone is an important concern. To accurately assess the health burden of inhaling oily PM, it is necessary to determine the crude oil content of the PM and to evaluate for size-dependence. In response to this public health concern, we characterized the total mass and crude oil content of $PM_{2.5}$ emitted from seawater contaminated by an oil slick with and without dispersant as a function of particle size. In order to complete this, a method utilizing a gas chromatography/mass spectrometer (GC/MS) was developed for effective extraction of *n*-alkanes from fibrous filters. Experiments were then split into two parts: 1) $PM_{2.5}$ sampling for gravimetric and chemical analyses to determine the mass fractions of the crude oil and dispersant and 2) size-fractioned PM sampling using a low-pressure cascade impactor to estimate the mass fraction of crude oil and dispersant as a function of particle size.

2. Methods

2.1. Experimental setup

Aerosols were generated by bubble bursting in a vertical tank made of thick, clear acrylic material (L = 0.3, W = 0.3, and H = 0.7 m) as shown in Fig. 1. The seawater was made artificially from aquarium sea salt (Instant Ocean®, Aquarium Systems, Blacksburg, VA, USA) mixed with tap water to maintain a salinity of 33 ppt. Throughout each experiment (3 h or 5 h), a bubble plume was continuously generated by injecting water/air at controlled flow rates into a shear-based nozzle. As described by Sampath et al. (2019), volumetric flow rates of air and water were maintained at 20 ± 0.4 cm^3/min and 13 ± 2 cm^3/min to generate mean bubble diameter of 614 μm. Uniformity of the bubble sizes can be verified by considering the equivalent bubble mode size that was 595 μm (3% smaller than the mean size). All bubbles rose to the water surface and eventually burst as described by Sampath et al. (2019).

The common diameter of bubbles produced by a breaking wave or whitecap in oceanic processes ranges from 68 μm to 2.4 mm (Cartmill and Su, 1993), which covers the average bubble size selected in the present study. The bubble mode size of 614 μm is also greater than the threshold determined by Blanchard and Syzdek (1988) for formation of film droplets. Previous study by Sampath et al. (2019) revealed that formation of film droplets is critical in generation of the nano-sized PM.

Aerosol sampling was conducted in two separate phases: 1) the vertical tank was equipped with a $PM_{2.5}$ sampler and 2) the vertical tank was equipped with a low pressure cascade impactor (LP-20,

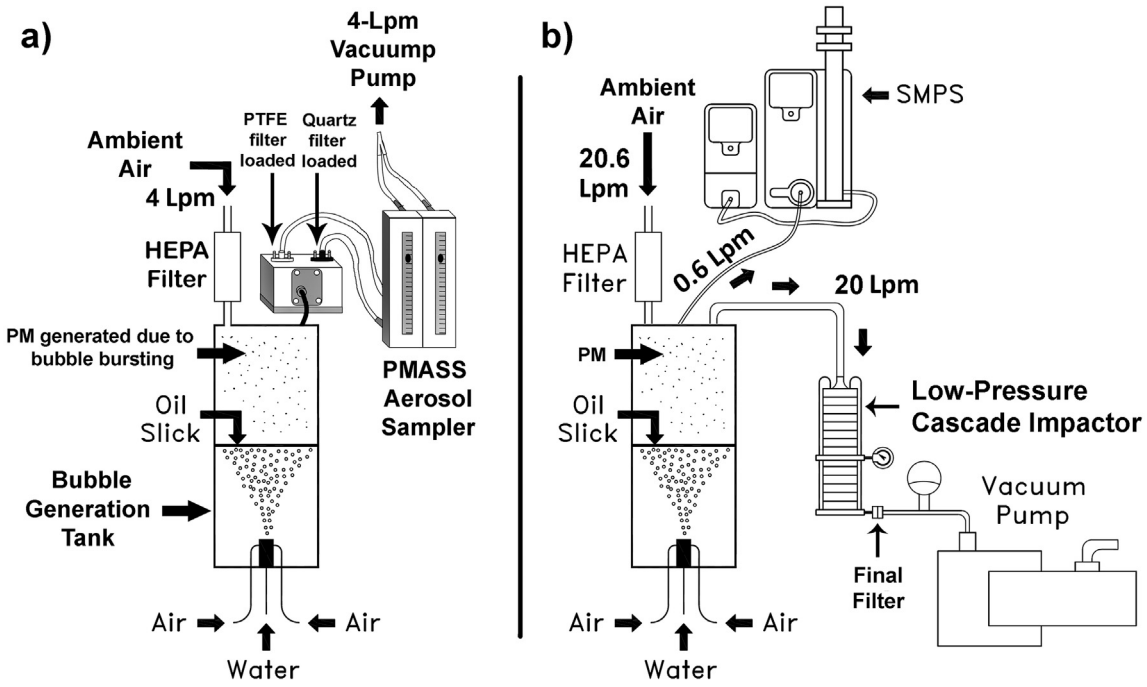

Fig. 1. Schematic of the experimental setup and sampling devices: a) using PMASS sampler for $PM_{2.5}$ and b) using the cascade impactor for size-fractioned sampling.

Dylec Co., Tokyo, Japan). In each phase, four experimental scenarios were considered: 1) uncontaminated seawater, 2) seawater with a slick of crude oil, 3) seawater with a slick of crude oil mixed with dispersant at a DOR 1:100, and 4) seawater with a slick of crude oil mixed with dispersant at a dispersant to oil ratio of 1:25 (DOR 1:25). In the last two experimental scenarios, the mixtures of dispersant and crude oil were mixed at the volumetric ratio of either 1:100 or 1:25 to form a total volume of 45 mL. The mixture was stirred for 10 s, then delicately poured onto the water surface to form the 0.5-mm slick. DOR 1:25 is within the range recommended by the United States Environmental Protection Agency (US EPA) of 1:10 to 1:50 (USEPA, 1995), and DOR 1:100 is close to the DOR utilized during Deepwater Horizon oil ridge blowout for underwater dispersion of the crude oil near the wellhead (DOR 1:130, OSAT/NOAA, 2010). The crude oil and dispersant were non-weathered Louisiana Light Sweet crude oil (MC252 surrogate) and Corexit 9500A (Nalco Environmental Solution LLC., Sugar Land, TX, USA), respectively. At the beginning of each experiment, the seawater level was controlled so that the headspace was 31.5 L. The water level was maintained by draining and injecting water as necessary.

2.2. Sampling procedure

Accurate quantification of organic PM compounds requires a laboratory procedure that recovers petrochemical compounds over a wide range of volatilities and polarities. For this purpose, the method developed by Swartz et al. (2003) was modified through selection of the most appropriate filter material and solvent for optimal extraction of *n*-alkanes in a wide range of C_{12}–C_{40}. This is an ideal range for detection of aerosolized hydrocarbon PM in this study in that molecular dynamic simulations by Liyana-Arachchi et al. (2014) showed C15 to C30 *n*-alkanes have the greatest likelihood of aerosolization due to bubble bursting. Quartz was found to be the preferred filter material for extraction, but the brittleness of baked quartz filters makes them susceptible to loss of mass during handling, which is not suitable for gravimetric analysis. Additional details on the semi-volatile and organic PM extraction from fibrous filters can be found in Swartz et al. (2003). A Personal Micro-environmental Aerosol Speciation Sampler (PMASS), developed by Demokritou et al. (2001), facilitates parallel sampling of the aerosol onto two separate filters. The PMASS is designed for 25-mm filters to collect aerosol at a total flow rate of 4 L/min (2 L/min per sampling column). One sampling column of the PMASS was loaded with a polytetrafluoroethylene (PTFE) membrane (Teflo® R2PI025, Pall Co., NY, USA) filter for gravimetric analysis. This 30-μm-thick filter that consists of multiple fibrous layers with nominal pore size of 3 μm and is a common filter used in $PM_{2.5}$ sampling (Boman et al., 2009; Bell et al., 2013; Gorbunov et al., 2013). The $PM_{2.5}$ mass was measured on a microbalance (model MX5, Mettler Toledo, Columbus, OH, USA) at a precision of 1-μg following a 4 h equilibration in a temperature- and humidity-controlled room ($T = 21 \pm 3$ °C and $RH = 30 \pm 2\%$). The second sampling column of the PMASS was loaded with a baked quartz membrane filter (LOT No.: 20492, Pall Co., NYC, NY, USA) to collect the particles for subsequent chemical analysis. Quartz filters were pre-baked at 550 °C for 6 h. To compensate for the loss of air inside the chamber due to sampling at 4 L/min, aerosol-free ambient air cleaned by a high-efficiency particulate air (HEPA) filter was injected into the tank at 4 L/min (See Fig. 1a). Each case was repeated in triplicate.

In the second phase of the study, the cascade impactor was utilized to collect PM in multiple size bins. The cascade impactor used in this study had 13 stages and required a flow rate of 20 L/min. The first 8 stages of the impactor, designed for collecting PM > 0.52 μm, operated at an atmospheric air pressure of 760 mmHg, but the last 5 stages, designed for collecting PM < 0.52 μm, operated under an air pressure range of 210–685 mmHg (Endo et al., 2003). To overcome the pressure drop, a rotary-vane vacuum pump with 0.75 hp of power (Model 1023, Gast Manufacturing Inc., Benton Harbor, MI, USA) was used. For the above-mentioned flow rate and air pressure conditions, the bin midpoint diameters of the coarse size stages were 12.1, 8.5, 5.7, 3.9, 2.5, 1.25, 0.76, and 0.52 μm. The 50% cutoff diameters of the low-pressure section of the sampler were 330, 220, 130, 60 nm. Filters

loaded into the cascade impactor were 81 mm in diameter and made of baked quartz fibers (Model TE-20-301-QZ, Tisch Environmental Co., Village of Cleves, OH, USA).

Continuous monitoring of the PM total mass concentrations and particle size distributions (PSD) was performed using a scanning mobility particle sizer (SMPS model 3938 with an electrostatic classifier model 3082 and a condensation particle counter model 3787, TSI Inc., Shoreview, MN, USA). This system had an inlet impactor with a cutoff diameter of 0.59 μm and operated at a flow rate of 0.6 L/min to measure nano-sized PM with electrical mobility diameters ranging from 10 to 370 nm every 63 s. In order to collect enough PM mass on each filter to surpass the GC/MS limit of detection (LOD) for crude oil and dispersant markers, the last three filters in the submicron range of the cascade impactor were combined into three size ranges of 60–130 nm, 130–330 nm, and 330–520 nm. Two additional blank filters were analyzed for correcting the results for baseline and environmental contaminations. The blank filters were not used for sampling and were kept in the weighing room. The mass concentrations on the blank filters were subtracted from the sample filter mass concentrations when estimating the relevant concentrations. To compensate for the sampling flow rates of 20 L/min by the cascade impactor and 0.6 by the SMPS, aerosol-free ambient air cleaned by a HEPA filter was injected into the top of the tank at 20.6 L/min (See Fig. 1b). The size-resolved experiments were performed one time each. Before each experiment, the tank was cleaned and rinsed multiple times and then flushed with clean air until the SMPS did not count any particles.

2.3. Chemical analysis protocol

2.3.1. GC/MS settings

Chromatographic analysis was done using a Trace GC-Ultra gas chromatograph attached to a Thermo ISQ Mass Spectrometer (GC/MS) with a 30 m × 0.25 mm (internal diameter) column and 0.25 μm film thickness (Rtx-1301Sil MS, Restek Inc., Bellefonte, PA, USA). The temperature ramp started at 80 °C, followed by a 2 min hold and an 8 °C/min increase to 200 °C. The final temperature ramped to 250 °C at 25 °C/min. The split/splitless injector was set to 250 °C with a split flow of 1.0 mL/min with helium as the carrier gas. All samples were analyzed using selected ion monitoring (SIM) mode.

2.3.2. Identification of the crude oil and dispersant markers

GC/MS analyses conducted on spiked samples of crude oil and dispersant revealed that dodecane and 1-(-2butoxy-1-methylethoxy)-2-propanol (BMEP) exhibited the highest peak areas on the GC/MS chromatograms, respectively. BMEP as a marker for dispersant Corexit 9500A has also been verified by Hayworth and Clement (2012).

2.3.3. Preparation of the samples

Extraction of the collected mass from a filter requires a solvent with a low polarity index and a high miscibility for interactions with hydrocarbons. Therefore, *n*-pentane (>98% GC grade, Thermo Fisher Scientific Inc., Waltham, MA, USA) with a polarity index of 0 and a high miscibility for dodecane was selected for extraction of *n*-alkane compounds from the PM filters (Richardson and Miiller, 1982). Extraction of the particles was performed following the method in Raksit and Punani (1997) for GC/MS detection of aliphatic glycol as a marker for dispersant. The LODs of dodecane and BMEP were determined by pipetting 100 μL of either pure crude oil or a mixture of crude oil and dispersant (DOR 1:100 and 1:25) on each filter diluted with deionized water. For each tracer, a 6-point calibration curve was generated from 0.005 to 0.2 μg/mL. Serial dilution factors of $1{:}10^1$, $1{:}10^2$, $1{:}10^3$, $1{:}10^4$, and $1{:}10^5$ of dodecane and BMEP were provided separately using pentane as the solvent. Then, solution concentrations of 0.005, 0.01, 0.02, 0.05, 0.1, and 0.2 μg/mL of either dodecane or BMEP in pentane were injected into the GC/MS to obtain the calibration curves.

The contaminated filters were left to dry for 1 h before they were transferred to polypropylene conical tubes. Each 25-mm filter was placed in a 15 mm tube, and 8 mL deionized water was added into each tube. The tubes were vortexed for 1 min and then shaken at 300 rpm for 15 min using an orbital shaker (IKA® Inc., Model KS 260 Basic, Staufen, Germany). Afterwards, a 1 mL aliquot of n-pentane was added to the tube and vortexing and shaking were repeated. Finally, a sample of 200 μL was collected from each tube and pipetted into inserts for chemical analysis by the GC/MS. For extraction of PM from 81-mm filters, each filter was placed in a 50-mL tube filled with 45 mL of deionized water and a 5 mL aliquot of n-pentane was added. The extraction efficiencies (η_{Dodecane} and η_{BMEP}) were defined by Eq. (1):

$$\eta_{\,Dodecane} \text{ or } \eta_{\,BMEP} = \frac{M_{CF} - M_{BF}}{M_P} \tag{1}$$

where M_{CF} refers to either the dodecane or BMEP mass derived from a filter spiked with a droplet of crude oil- or dispersant-pentane, M_{BF} refers to either dodecane or BMEP derived from a blank filter, and M_P refers to the mass of either dodecane or BMEP from direct injection of either crude oil or dispersant, respectively.

2.3.4. Estimation of the concentrations of PM constituents

Each gravimetrically-analyzed PTFE filter corresponded to a quartz filter used for the GC/MS analysis to estimate the dodecane and BMEP concentrations of the collected PM. For the chemical analysis conducted in this study, the total mass of collected airborne dodecane or BMEP depended on the total volume of solvent and extraction efficiency of dodecane or BMEP from the quartz filters. The crude oil and dispersant fractions of the sampled PM2.5 (CCrude oil and CDispersant) were calculated using Eqs. (2) and (3):

$$C_{Crude\ oil} = \left[\frac{1}{\eta_{\,Dodecane}} \times \rho_{Dodecane} \times \frac{1}{k_{\,Dodecane/Crude\ oil}} \times \frac{V_{Solvent}}{V_{Total\ air}} \right] \tag{2}$$

$$C_{Dispersant} = \left[\frac{1}{\eta_{\,BMEP}} \times \rho_{BMEP} \times \frac{1}{k_{\,BMEP/Dispersant}} \times \frac{V_{Solvent}}{V_{Total\ air}} \right] \tag{3}$$

where $V_{Solvent}$ denotes the volume of added pentane for extraction of non-polar dodecane or BMEP from the quartz filters, $\rho_{Dodecane}$ and ρ_{BMEP} denote the calculated concentrations in the analyzed volume of the solvent, $V_{Total\ air}$ denotes the total volume of the sampled air, and $k_{Dodecane/Crude\ oil}$ and $k_{BMEP/Dispersant}$ denote volumetric concentrations of dodecane in crude oil and BMEP in the dispersant, respectively. $k_{Dodecane/Crude\ oil}$ and $k_{BMEP/Dispersant}$ were calculated through GC/MS analysis of dodecane in 100 μL samples of crude oil and BMEP in 100 μL samples of dispersant.

3. Results

3.1. Phase I: mass concentration and chemical analysis of $PM_{2.5}$

The extraction efficiency of dodecane or BMEP on the $PM_{2.5}$ filters were 88 and 81% for 0.01 μg/mL of injected crude oil and dispersant, respectively, and 83 and 79% for 0.1 μg/mL of injected crude oil and dispersant, respectively. On average, 1.5 ± 0.4% of the

crude oil volume consisted of dodecane ($k_{Dodecane/Crude\ oil}$), and the average content of BMEP in the dispersant sample ($k_{BMEP/Dispersant}$) was 59.8 ± 3.8%.

The $PM_{2.5}$ mass concentration results are summarized in Table 1. All DOR 1:25 experiments resulted in the highest concentrations (20.83 ± 5.2 μg/m^3), and the three experiments with a slick of pure crude oil resulted in the lowest $PM_{2.5}$ concentration (2.37 ± 1.07 μg/m^3). The average dodecane concentration of $PM_{2.5}$ from pure crude oil was 11.3 ng/m^3. For the calculated crude oil and dispersant concentrations based on Eqs. (2) and (3), the increase in the average $PM_{2.5}$ concentration from DOR 1:25 was 8.83 times greater than from pure crude oil (20.83 vs 2.36 μg/m^3). By decreasing the DOR from 1:25 to 1:100, the increase factor was only 4.59 (10.83 vs 2.36 μg/m^3). The coefficient of variation (CV) for the total $PM_{2.5}$ mass concentration were greater than 8% indicating a relatively high variability per run.

Estimated concentrations of crude oil and dispersant from the $PM_{2.5}$ samples for each slick scenario are displayed in Fig. 2. While the percentage of crude oil in $PM_{2.5}$ decreased from 32.6% to 8.3% when 1:25 volume of dispersant was added, the average crude oil concentration for the crude oil only slick (0.77 μg/m^3) increased by 2.37 times when dispersant was added (1.17 times at DOR 1:100). The aerosolized crude oil in $PM_{2.5}$ for DOR 1:25 and DOR 1:100 were similar at 8.3 and 8.8%, respectively. The dispersant concentration in all cases were negligible and did not exceed 10 ng/m^3. In the gravimetric analyses, the pure crude oil scenario exhibited the highest variability across replicated experiments (44%). However, increasing the dispersant concentration resulted in an increase in the variability of the estimated aerosolized crude oil and dispersant concentrations (crude oil and dispersant CVs of 8% at DOR 1:25 and crude oil and dispersant CVs of 6 and 4% at DOR 1:100, respectively).

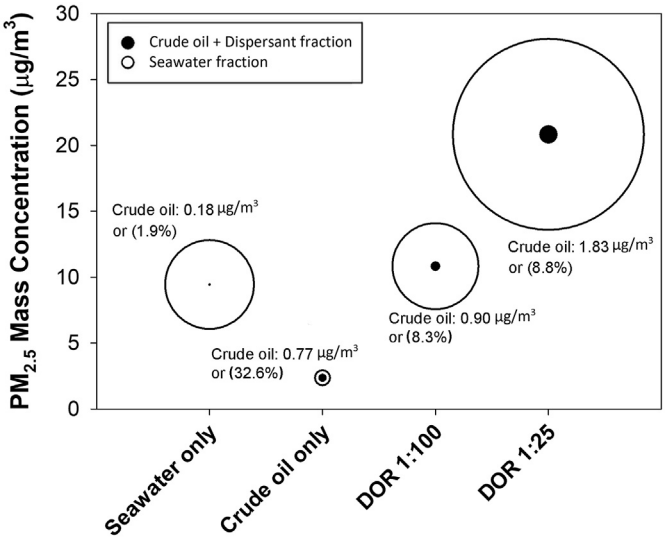

Fig. 2. Physical and chemical analyses of the total $PM_{2.5}$ concentrations and crude oil fractions for the four scenarios averaged over 3-hr of sampling. The hollow circles denote the $PM_{2.5}$ mass concentrations, and the black circles denote the crude oil content of the aerosol. The values in parenthesis indicate the percentage of crude oil within the $PM_{2.5}$ mass concentration that is displayed as the area of black circle within the whole area of hollow circle.

3.2. Phase II: size-fractioned chemical analysis of PM

The average mass concentrations of crude oil and dispersant resulting from the different slick scenarios at different particle sizes are compared in Fig. 3. The chemical analysis of the filters showed that the mixture slicks (DOR 1:25 or DOR 1:100) resulted in greater concentrations of crude oil compared to the case with pure crude oil slick at two particle size bins (<220 nm and 330–520 nm). For instance, the estimated crude oil concentration for $d_p < 220$ nm was 647 ng/m^3 for DOR 1:25, which decreased to 285 ng/m^3 for DOR 1:100. These are both greater than the slick of pure crude oil (111 ng/m^3). The increase in aerosolized crude oil mass with increasing dispersant was not consistent across size fractions. For instance, for particles larger than 2.5 μm, increasing the ratio from DOR 1:100 to DOR 1:25 did not lead to a notable increase in the aerosolized crude oil concentration, but increase in the dispersant ratio from 1:100 to 1:25 for $d_p < 220$ nm particles led to 2.26 times increase in aerosolized crude oil. The greatest increase in the mass of aerosolized crude oil was related to particles with $d_p < 220$ nm. The total amount of dispersant added did not exceed 2 mL and the estimated dispersant concentrations were relatively low (<6 ng/m^3 for particles between 0.9 and 1.4 μm) and were not conclusively different across different size bins.

3.3. Total concentration and particle size distribution of PM

The total concentrations and particle size distributions of the aerosolized droplets are displayed in Fig. 4. Compared to the bursting bubble PSD reported by Sampath et al. (2019), similar particle mode sizes (70–130 nm) for all four slick scenarios were observed in our study. The greatest number of aerosolized particles was observed from the slick of mixed crude oil and dispersant (DOR 1:25) with about 100 cm^{-3} at a particle mode size of 95 nm. The pure crude oil slick resulted in the lowest number of aerosolized particles, also observed by Sampath et al. (2019). The decreased particle number concentration from crude oil only slicks compared to the seawater only experiment is likely due to the increase in viscosity. Interestingly, all four scenarios presented a negligible difference in the total number of airborne droplets for particles smaller than 30 nm.

4. Discussion

4.1. $PM_{2.5}$ mass concentrations

The average $PM_{2.5}$ concentration when there was no

Table 1
$PM_{2.5}$ mass concentrations and crude oil and dispersant concentrations averaged over three replicated experiments of each slick type.

Slick type	Total $PM_{2.5}$		Crude oil		Dispersant	
	Mean (μg/m^3)	CV[a] (%)	Mean (μg/m^3)	CV (%)	Mean (μg/m^3)	CV (%)
Clean seawater (no slick)	9.44	24	0.18	4	<LOD[b]	–
Crude oil only	2.36	44	0.77	8	<LOD	–
DOR 1:25	20.83	25	1.83	8	7.21×10^{-3}	8
DOR 1:100	10.83	8	0.90	6	1.02×10^{-3}	4

[a] Coefficient of variation: the ratio of the standard deviation to the mean in percentage.
[b] LOD: Limit of detection for measurements of $\rho_{Dodecane}$ and ρ_{BMEP} were 10 and 1 ng/m^3, respectively.

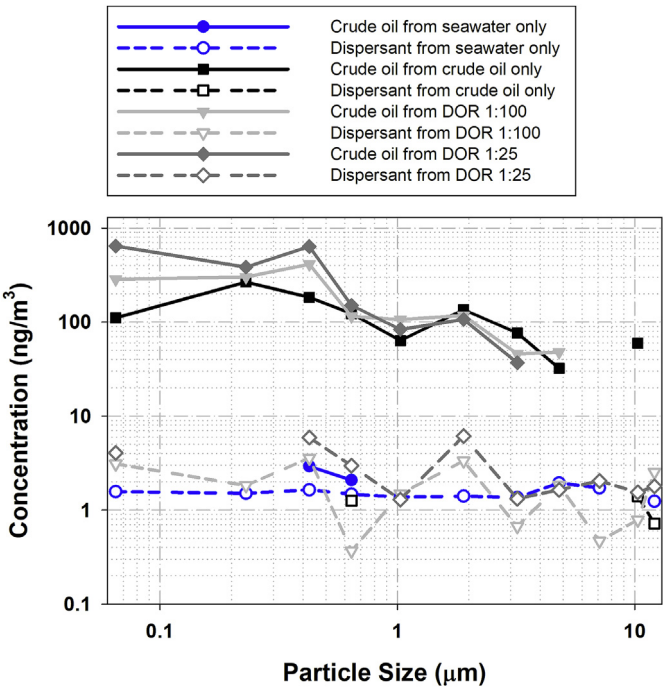

Fig. 3. Size-dependent average mass concentrations of crude oil and dispersant estimated based on chemical analysis of the cascade impactor filters for the four scenarios. Stages finer than 220 nm were aggregated in order to exceed the detection limit.

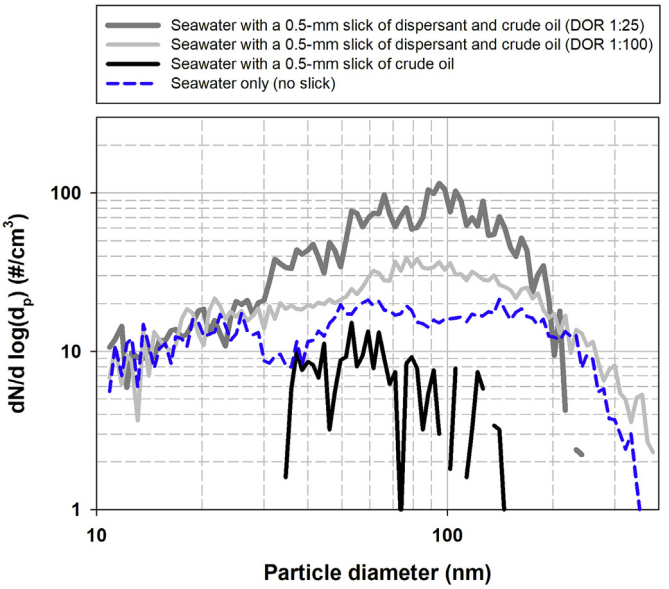

Fig. 4. Particle size distributions averaged over a 3 h experiment for the four contamination scenarios. Sampling was conducted using a scanning mobility particle sizer instrument.

contamination on the seawater was 9.44 μg/m^3, which decreased to 2.36 μg/m^3 (about 4 times smaller) in the presence of a crude oil slick. This observation agrees with findings by Sampath et al. (2019). In the present study, an increase in the dispersant concentration yielded a greater total mass of airborne crude oil droplets (20.83 μg/m^3 at DOR 1:25 and 10.83 μg/m^3 at DOR 1:100). These concentrations are equivalent to increase factors of 8.83 and 4.59, respectively, which suggests that the relationship between DOR and the mass of airborne crude oil content was not linear. Sampath et al. (2019) also reported 3.39 times increase for airborne particles with an aerodynamic diameter smaller than about 25 μm in the DOR 1:25 scenario (Sampath et al., 2019).

4.2. Chemical analysis of fine PM

4.2.1. $PM_{2.5}$ samples

Although the total volume of crude oil in the tank for all cases, except seawater only (no slick), were comparable, the crude oil concentration in the airborne $PM_{2.5}$ was not the same. The greatest air concentration of crude oil (1.83 μg/m^3) was measured during the DOR 1:25 experiment, as summarized in Table 1. This implies that adding dispersant to a contamination slick led to an increase (2.37 times) of the crude oil concentration in the airborne droplets compared to pure crude oil even though the total volume of oil was slightly decreased (because a fraction of the slick volume is dispersant). For DOR 1:100, the average crude oil concentration (0.90 μg/m^3) was slightly higher (1.17 times) than the case with a slick of pure crude oil (0.77 μg/m^3 as seen in Table 1 and Fig. 2). The dispersant to oil ratio in $PM_{2.5}$ airborne droplets for the DOR 1:25 (0.04) and DOR 1:100 scenarios (0.01) was 0.039 and 0.011, respectively. This indicates the proportion of dispersant to oil in the seawater and in the atmosphere was similar.

4.2.2. Size-fractioned samples of PM

The PSD plots displayed in Fig. 4 demonstrated that the statistical mode size of the aerosolized particles in all slick cases was below 100 nm. Considering the plot for DOR 1:25 displayed in Fig. 4, the area under the curve is equal to the total number of particles smaller than 370 nm. Assuming an average density of 0.8 g/cm^3 for crude oil, a total mass concentration of about 620 ng/m^3 was estimated. The total mass concentration of crude oil and dispersant based on the cascade impactor filters for $d_p < 220$ nm for DOR 1:25, yielded a similar mass concentration value of 649 ng/m^3. However, the impact of adding dispersant to increasing mass concentration of aerosolized crude oil PM was highly dependent on the particle size, which could not be resolved for particles smaller than 220 nm. Therefore, it is expected that the increased PM mass concentration ratios containing crude oil would be even greater than 8.6 (the ratio of dodecane concentration from DOR 1:25 to pure crude oil) when considering only particles smaller than 220 nm.

4.3. Limitations

The crude oil and dispersant tested in this study were freshly drawn from the barrel. Bacosa et al. (2015) investigated the impact of weathering of Light Louisiana Sweet crude oil and reported biodegradation and photooxidation rates for hydrocarbons based on their number of benzene rings. Their results showed that adding a dispersant expedites degradation of *n*-alkanes but it is less effective in degradation of polycyclic aromatic hydrocarbons (PAHs), as photooxidation contributed to about 70% of the PAHs degradation. Furthermore, the lack of nutrients in the tested water might greatly hinder biodegradation (Personna et al., 2014; Pan et al., 2017) that consequently impact aerosolization of the fine PM in the real-world waterbodies. Aging of crude oil, with and without adding dispersant, may alter dodecane and BMEP PM concentrations from bubble bursting. The apportionment of crude oil constituents, which are non-volatile, before and after aerosolization has been assumed to be the same. This means dodecane, with an average initial volumetric fraction of 1.5%, was assumed to maintain its proportion for all aerosolized droplets. Furthermore, aerosol concentration, particle size distribution, and chemical

composition of the aerosolized droplets may be altered when seawater minerals and different water salinities are present. Therefore, using natural seawater containing minerals at different water salinities is suggested for future work.

Furthermore, cascade impactors can also promote loss of semi-volatile species mass due to evaporation caused by large pressure drops (Furuuchi et al., 2010). These experiments required hours of operation in order to collect adequate mass for quantitative chemical analysis, which may have resulted in loss of semi-volatile species. This also introduces uncertainty in the conversion from dodecane concentration to the total crude oil mass.

The slick within the experimental chamber cannot spread naturally as it does over the ocean; resulting in aerosols that are concentrated in a small air space within the chamber. Measurement of $PM_{2.5}$ concentrations and estimation of the crude oil content for different particle sizes was limited to a pilot-scale setup at a close distance to the water surface. In the real-world scenario, dilution imposed by natural processes such as winds will result in different concentrations at further distances (both horizontally and vertically) from the contaminated surface. While estimated concentrations may differ at further distances from the surface, given the large proportion of particles in the submicron size that is not dominated by gravitational settling, the observed trend of an increase in the crude oil content of $PM_{2.5}$ with an increase in the dispersant content is likely to persist at different heights above the surface. Therefore, the results of this study can be used as emission rates for additionally modeling to consider real-world exposures and potential health risk characterization of on-boat cleanup workers along with water surface-dwelling birds and mammals. To better quantify such an impact, field measurement or numerical modeling studies are recommended.

5. Conclusions

We demonstrated that adding a dispersant onto a crude oil slick increases the airborne crude oil content. At a dispersant to oil ratios of 1:25 and 1:100, there was 8.83 and 4.59 times increase in the total mass of emitted $PM_{2.5}$ compare to a slick of only crude oil. The average aerosolized crude oil concentration from a pure crude oil slick was 0.77 $\mu g/m^3$, which increased 2.37 times when the dispersant (DOR 1:25) was added (1.17 times at DOR 1:100). We observed a similar trend for UFP. The estimated concentration of crude oil for $d_p < 220$ nm was 644 ng/m^3 for DOR 1:25 and 285 ng/m^3 for DOR 1:100, which are both greater than 111 ng/m^3 from pure crude oil. We found that the crude oil concentration within the PM was highly dependent on the particle size. However, the fraction of crude oil within the total aerosolized $PM_{2.5}$ mass increased about 4 times when the dispersant fraction increased by 4 times, suggesting a linear relationship. We attribute the significantly increased crude oil concentration in $PM_{2.5}$ after the dispersant was added to increased UFP concentrations, which is a health concern because UFP are more effectively transported into the lower respiratory tract of humans (and possible other animals). We recommend decreasing the DOR when treating an oil spills as a strategy for mitigating adverse health impacts and maintaining accurate control of DOR when dispersants are used.

Declaration of competing interest

The authors declare the following financial interests/personal relationships which may be considered as potential competing interests: All authors decline any conflict of interests (both as a financial interest or as personal relationships with the people involved in this research topic or affected by this study).

CRediT authorship contribution statement

Nima Afshar-Mohajer: Writing - review & editing, Conceptualization, Methodology, Formal analysis, Visualization, Writing - original draft. **Andres Lam:** Formal analysis, Writing - review & editing. **Lakshmana Dora:** Methodology, Resources. **Joseph Katz:** Supervision, Conceptualization, Resources, Writing - review & editing. **Ana M. Rule:** Supervision, Methodology, Resources, Writing - review & editing. **Kirsten Koehler:** Supervision, Conceptualization, Validation, Writing - review & editing.

Acknowledgments

This research was made possible by a grant from the Gulf of Mexico Research Initiative (GoMRI). Authors are thankful to Dr. Misti Levy Zamora for her insights and help reviewing the manuscript. Data are publicly available through the Gulf of Mexico Research Initiative Information & Data Cooperative (GRIIDC) at https://data.gulfresearchinitiative.org (doi: <10.7266/n7-rte4-s004> and <10.7266/N 77H1GZG>). Authors are grateful to Dr. Jana Kesavan for use of the cascade impactor.

References

Afshar-Mohajer, N., Li, C., Rule, A.M., Katz, J., Koehler, K., 2018. A laboratory study of particulate and gaseous emissions from crude oil and crude oil-dispersant contaminated seawater due to breaking waves. Atmos. Environ. 179, 177–186.
Afshar-Mohajer, N., Fox, M.A., Koehler, K., 2019. The human health risk estimation of inhaled oil spill emissions with and without adding dispersant. Sci. Total Environ. 654, 924–932.
Aguilera, F., Méndez, J., Pásaro, E., Laffon, B., 2010. Review on the effects of exposure to spilled oils on human health. J. Appl. Toxicol. 30, 291–301.
Avens, H.J., Unice, K.M., Sahmel, J., Gross, S.A., Keenan, J.J., Paustenbach, D.J., 2011. Analysis and modeling of airborne BTEX concentrations from the Deepwater Horizon oil spill. Environ. Sci. Technol. 45, 7372–7379.
Bacosa, H.P., Erdner, D.L., Liu, Z., 2015. Differentiating the roles of photooxidation and biodegradation in the weathering of Light Louisiana Sweet crude oil in surface water from the Deepwater Horizon site. Mar. Pollut. Bull. 95, 265–272.
Bell, S.W., Hansell, R.A., Chow, J.C., Tsay, S.C., Hsu, N.C., Lin, N.H., Wang, S.H., Ji, Q., Li, C., Watson, J.G., Khlystov, A., 2013. Constraining aerosol optical models using ground-based, collocated particle size and mass measurements in variable air mass regimes during the 7-SEAS/Dongsha experiment. Atmos. Environ. 78, 163–173.
Blanchard, D.C., Syzdek, L.D., 1988. Film drop production as a function of bubble size. J. Geophys. Res. 93, 3649–3654.
Boman, J., Gatari, M.J., Janhäll, S., Shannigrahi, A.S., Wagner, A., 2009. Elemental content of PM 2.5 aerosol particles collected in Göteborg during the Göte-2005 campaign in February 2005. Atmos. Chem. Phys. 9 (7).
Boylan, D.B., Tripp, B.W., 1971. Determination of hydrocarbons in seawater extracts of crude oil and crude oil fractions. Nature 230, 44.
Cartmill, J.W., Su, M.Y., 1993. Bubble size distribution under saltwater and freshwater breaking waves. Dynam. Atmos. Oceans 20, 25–31.
D'Andrea, M.A., Reddy, G.K., 2013. Health consequences among subjects involved in Gulf oil spill clean-up activities. Am. J. Med. 126, 966–974.
De Leeuw, G., Andreas, E.L., Anguelova, M.D., Fairall, C.W., Lewis, E.R., O'Dowd, C., et al., 2011. Production flux of sea spray aerosol. Rev. Geophys. 49, RG2001.
Demokritou, P., Kavouras, I.G., Ferguson, S.T., Koutrakis, P., 2001. Development and laboratory performance evaluation of a personal multipollutant sampler for simultaneous measurements of particulate and gaseous pollutants. Aerosol Sci. Technol. 35, 741–752.
Endo, O., Sugita, K., Goto, S., Amagai, T., Matsushita, H., 2003. Mutagenicity of size-fractioned airborne particles collected with Andersen low pressure impactor. J. Health Sci. 49, 22–27.
Ehrenhauser, F.S., Avij, P., Shu, X., Dugas, V., Woodson, I., Liyana-Arachchi, T., Valsaraj, K.T., 2014. Bubble bursting as an aerosol generation mechanism during an oil spill in the deep-sea environment: laboratory experimental demonstration of the transport pathway. Environ. Sci.: Process. Impact 16, 65–73.
Fuentes, E., Coe, H., Green, D., Leeuw, G.D., McFiggans, G., 2010. Laboratory-generated primary marine aerosol via bubble-bursting and atomization. Atmos. Meas. Tech. 3, 141–162.
Furuuchi, M., Eryu, K., Nagura, M., Hata, M., Kato, T., Tajima, N., et al., 2010. Development and performance evaluation of air sampler with inertial filter for nanoparticle sampling. Aerosol Air Qual. Res. 10, 185–192.
Gopalan, B., Katz, J., 2010. Turbulent shearing of crude oil mixed with dispersants generates long microthreads and microdroplets. Phys. Rev. Lett. 104, 054501.
Gorbunov, B., Muir, R., Jackson, P., Priest, N.D., 2013. Evaluation of the Airborne Particles Fraction Responsible for Adverse Health Effects (No. AECL-CW–121110-

CONF-033). Atomic Energy of Canada Limited.
Hanna, S.R., Drivas, P.J., 1993. Modeling VOC emissions and air concentrations from the Exxon Valdez oil spill. J. Air Waste Manag. Assoc. 43, 298–309.
Hayworth, J.S., Clement, T.P., 2012. Provenance of Corexit-related chemical constituents found in nearshore and inland Gulf Coast waters. Mar. Pollut. Bull. 64, 2005–2014.
Kim, K.H., Kabir, E., Kabir, S., 2015. A review on the human health impact of airborne particulate matter. Environ. Int. 74, 136–143.
Kleindienst, S., Paul, J.H., Joye, S.B., 2015. Using dispersants after oil spills: impacts on the composition and activity of microbial communities. Nat. Rev. Microbiol. 13, 388.
Lessard, R.R., DeMarco, G., 2000. The significance of oil spill dispersants. Spill Sci. Technol. Bull. 6, 59–68.
Levy, B.S., Nassetta, W.J., 2011. The adverse health effects of oil spills: a review of the literature and a framework for medically evaluating exposed individuals. Int. J. Occup. Environ. Health 17, 161–168.
Liyana-Arachchi, T.P., Zhang, Z., Ehrenhauser, F.S., Avij, P., Valsaraj, K.T., Hung, F.R., 2014. Bubble bursting as an aerosol generation mechanism during an oil spill in the deep-sea environment: molecular dynamics simulations of oil alkanes and dispersants in atmospheric air/salt water interfaces. Environ. Sci.: Process. Impact 16, 53–64.
Meo, S.A., Al-Drees, A.M., Meo, I.M., Al-Saadi, M.M., Azeem, M.A., 2008. Lung function in subjects exposed to crude oil spill into sea water. Mar. Pollut. Bull. 56, 8.
Merhi, Z.O., 2010. Gulf Coast oil disaster: impact on human reproduction. Fertil. Steril. 94, 1575–1577, 8-94.
Morita, A., Kusaka, Y., Deguchi, Y., Moriuchi, A., Nakanaga, Y., Iki, M., et al., 1999. Acute health problems among the people engaged in the cleanup of the Nakhodka oil spill. Environ. Res. 81, 185–194.
O'Dowd, C.D., De Leeuw, G., 2007. Marine aerosol production: a review of the current knowledge. Philos. Trans. Roy. Soc. A 365, 1753–1774.
Oberdörster, G., Oberdörster, E., Oberdörster, J., 2007. Concepts of nanoparticle dose metric and response metric. Environ. Health Perspect. 115. A290-A290.
Oil Tanker Spill Statistics, 2019. The International Tanker Owners Pollution Federation. http://www.itopf.org/knowledge-resources/data-statistics/statistics/.
OSAT/NOAA Report, 2010. Summary report for sub-sea and sub-surface oil and dispersant detection: sampling and monitoring. In: Operational Science Advisory Team (Multiagency). Washington, D.C (last consulted in April 26th, 2012). http://www.restorethegulf.gov/release/2011/07/29/osat-summary-report-sub-sea-and-sub-surface-oil-and-dispersant-detection-ecotoxicology.
Pan, Z., Personna, Y.R., Boufadel, M.C., King, T., Mason, J., Axe, L., Geng, X., 2017. Biodegradation of dispersed weathered endicott oil in Prince William sound water. J. Environ. Eng. 143, 04017044.
Personna, Y.R., King, T., Boufadel, M.C., Zhang, S., Kustka, A., 2014. Assessing weathered Endicott oil biodegradation in brackish water. Mar. Pollut. Bull. 86, 102–110.
Pope III, C.A., Dockery, D.W., 2006. Health effects of fine particulate air pollution: lines that connect. J. Air Waste Manag. Assoc. 56, 709–742.
Raksit, A., Punani, S., 1997. Gas chromatographic—mass spectrometric investigation of aliphatic glycols in environmental samples. J. Chromatogr. Sci. 35, 489–494.
Resch, F.J., Darrozes, J.S., Afeti, G.M., 1986. Marine liquid aerosol production from bursting of air bubbles. J. Geophys. Res.: Oceans 91, 1019–1029.
Richardson, J.S., Miiller, D.E., 1982. Identification of dicyclic and tricyclic hydrocarbons in the saturate fraction of a crude oil by gas chromatography/mass spectrometry. Anal. Chem. 54, 765–768.
Riehm, D.A., McCormick, A.V., 2014. The role of dispersants' dynamic interfacial tension in effective crude oil spill dispersion. Mar. Pollut. Bull. 8, 155–163.
Rosenberger, A.L.J., MacDuffee, M., Rosenberger, A.G., Ross, P.S., 2017. Oil spills and marine mammals in British Columbia, Canada: development and application of a risk-based conceptual framework. Arch. Environ. Contam. Toxicol. 73, 131–153.
Rundell, K.W., Hoffman, J.R., Caviston, R., Bulbulian, R., Hollenbach, A.M., 2007. Inhalation of ultrafine and fine particulate matter disrupts systemic vascular function. Inhal. Toxicol. 19, 133–140.
Sampath, K., Afshar-Mohajer, N., Chandrala, L.D., Heo, W.-S., Gilbert, J., Austin, D., Koehler, K., Katz, J., 2019. Aerosolization of crude oil-dispersant slicks due to bubble bursting. J. Geophys. Res. Atmos. 124, 5555–5578.
Schulz, H., Harder, V., Ibald-Mulli, A., Khandoga, A., Koenig, W., Krombach, F., et al., 2005. Cardiovascular effects of fine and ultrafine particles. J. Aerosol Med. 18, 1–22.
Sellegri, K., O'Dowd, C.D., Yoon, Y.J., Jennings, S.G., de Leeuw, G., 2006. Surfactants and submicron sea spray generation. J. Geophys. Res.: Atmosphere 111 (D22).
Sim, M.S., Jo, I.J., Song, H.G., 2010. Acute health problems related to the operation mounted to clean the Hebei Spirit oil spill in Taean, Korea. Mar. Pollut. Bull. 60, 51–57.
Spiel, D.E., De Leeuw, G., 1996. Formation and production of sea spray aerosol. J. Aerosol Sci. 27, S65–S66.
Spiel, D.E., 1997. A hypothesis concerning the peak in film drop production as a function of bubble size. J. Geophys. Res.: Oceans 102 (C1), 1153–1161.
Swartz, E., Stockburger, L., Gundel, L.A., 2003. Recovery of semivolatile organic compounds during sample preparation: implications for characterization of airborne particulate matter. Environ. Sci. Technol. 37, 597–605.
Takeshita, R., Sullivan, L., Smith, C., Collier, T., Hall, A., Brosnan, T., Rowles, T., Schwacke, L., 2017. The Deepwater Horizon oil spill marine mammal injury assessment. Endanger. Species Res. 33, 95–106.
Talbott, E.O., Xu, X., Youk, A.O., Rager, J.R., Stragand, J.A., Malek, A.M., 2011. Risk of leukemia as a result of community exposure to gasoline vapors: a follow-up study. Environ. Res. 111, 597–602.
Ulevicius, V., Willeke, K., Grinshpun, S.A., Donnelly, J., Lin, X., Mainelis, G., 1997. Aerosolization of particles from a bubbling liquid: characteristics and generator development. Aerosol Sci. Technol. 26, 175–190.
United States Environmental Protection Agency, 1995. https://www.epa.gov/emergency-response/corexittm-ec9500a.
Valavanidis, A., Fiotakis, K., Vlachogianni, T., 2008. Airborne particulate matter and human health: toxicological assessment and importance of size and composition of particles for oxidative damage and carcinogenic mechanisms. J. Environ. Sci. Health C 26, 339–362.
Venkataraman, P., Tang, J., Frenkel, E., McPherson, G.L., He, J., Raghavan, S.R., et al., 2013. Attachment of a hydrophobically modified biopolymer at the oil–water interface in the treatment of oil spills. ACS Appl. Mater. Interfaces 5, 3572–3580.
Veron, F., Hopkins, C., Harrison, E.L., Mueller, J.A., 2012. Sea spray spume droplet production in high wind speeds. Geophys. Res. Lett. 39, L16602.
Zhang, H., Khatibi, M., Zheng, Y., Lee, K., Li, Z., Mullin, J.V., 2010. Investigation of OMA formation and the effect of minerals. Mar. Pollut. Bull. 60, 1433–1441.
Zhao, L., Gao, F., Boufadel, M.C., King, T., Robinson, B., Lee, K., Conmy, R., 2017. Oil jet with dispersant: macro-scale hydrodynamics and tip streaming. AIChE J. 63, 5222–5234.